Martin Gromniak*, Maximilian Neidhardt, Axel Heinemann, Klaus Püschel and Alexander Schlaefer

Needle placement accuracy in CT-guided robotic post mortem biopsy

https://doi.org/10.1515/cdbme-2020-0031

Abstract: Forensic autopsies include a thorough examination of the corpse to detect the source or alleged manner of death as well as to estimate the time since death. However, a full autopsy may be not feasible due to limited time, cost or ethical objections by relatives. Hence, we propose an automated minimal invasive needle biopsy system with a robotic arm, which does not require any online calibrations during a procedure. The proposed system can be easily integrated into the workflow of a forensic biopsy since the robot can be flexibly positioned relative to the corpse. With our proposed system, we performed needle insertions into wax phantoms and livers of two corpses and achieved an accuracy of 4.34 ± 1.27 mm and 10.81 ± 4.44 mm respectively.

Keywords: biopsy; CT imaging; forensic autopsy; robotics.

Problem

Forensic autopsies include a thorough examination of the corpse to detect the source or alleged manner of death as well as to estimate the time since death. Often a conventional autopsy (CA) is not feasible due to time, cost or ethical objections by relatives. As a result, the number of autopsies performed has decreased in the last decade [1] although studies repeatedly state the necessity of quality control in treatment and diagnosis by CA [2].

Minimally invasive biopsies under CT guidance can offer an alternative to CA. These virtual autopsies (VA) have the advantage that probes of organs, cysts or even gases can be extracted at precise and documentable locations of the body and subsequently associated with the imaging.

In contrast, opening the corpse can lead to fluids being mixed or pathologic gases of interest (e.g. air embolism) escaping the body, which can in turn lead to inconclusive or false results. Moreover, a VA is time efficient which is critical due to cellular post mortem autolysis and decomposition. Hence, a simple and fast needle biopsy approach can secure samples as early as possible after death [3].

However, placing biopsy needles precisely and without a line of sight is time consuming and accuracy in needle placement is dependent on the experience of the physician. Hence, automated systems for tissue sample extraction with a robotic arm can be of valuable assistance to a medical examiner. Typically, a CT-scan of the corpse is performed and a medical examiner defines targets and needle trajectories for tissue biopsies which are of interest to him. Existing systems for image-guided needle placement involve custom-built robots which are rigidly attached to the CT table and only provide a rather small target volume [4, 5]. Examples for commercially available systems include MazorX (Medtronic) and iSYS1 (iSYS Medizintechnik, Fusion Robotics). However, those only align the needle with the patient and the physician advances the needle manually. Particularly designed for VA, the Virtobot system [6] offers a larger target volume but is dependent on a rigidly attached ceiling-mounted robot and the need for calibrating the robot's position prior to every puncture.

We present a robotic biopsy system that can be easily integrated into the workflow of a forensic autopsy. We use a custom co-registration marker, which is simply placed on top of the corpse prior to CT scanning, to register the CT image reference frame to the robot's workspace. The medical examiner defines a biopsy target and the needle path in the CT image. The final puncture is executed by a general purpose 7 degrees of freedom robot, which can be placed close to the corpse for needle

Martin Gromniak and Maximilian Neidhardt: contributed equally to this work.

***Corresponding author: Martin Gromniak**, Institute of Medical Technology and Intelligent Systems, Hamburg University of Technology, Hamburg, Germany, E-mail: Martin.Gromniak@tuhh.de
Maximilian Neidhardt and Alexander Schlaefer, Institute of Medical Technology and Intelligent Systems, Hamburg University of Technology, Hamburg, Germany
Axel Heinemann and Klaus Püschel, Department of Legal Medicine, Medical Center Hamburg-Eppendorf (UKE), Hamburg, Germany

punctures and then removed again. We report the accuracy of our system for needle placement in wax phantoms and in two corpses.

2 Material and methods

CT-guided needle placement involves a series of coordinate transformations and calibrations which are calculated prior to the needle puncture.

Experimental setup and calibration

Our experimental setup is depicted in Figure 1. It employs a robot (Panda, Franka Emika), a tracking camera (fusionTrack, Altracsys) and a custom-made co-registration marker (*CoReg*). The co-registration marker can be detected in the CT images and by the tracking camera and can therefore establish a transformation between these coordinate systems. It employs a CNC machined 5 × 5 pattern of steel balls (r=2 mm) equidistantly spaced at 20 mm which can be well detected in the CT images. Four reflective fiducials are attached to the phantom and represent a marker for the tracking system. The rigid transformation from reflective marker (RM) frame to CT marker (CTM) frame ${}^{\mathrm{RM_{CoReg}}}T_{\mathrm{CTM}}$ was obtained by recording the positions of the steel balls with a hand held stylus tracked by the tracking camera. We performed a hand-eye calibration between robot and tracking camera reference frame using another reflective marker attached to the end effector (EE) of the robot ($\mathrm{RM_{EE}}$). The calibration transformations were obtained with the QR24 algorithm [7] using 40 robot and camera poses. With the results of the hand-eye calibration, we calculated the rigid transform from the robot's base (B) to a marker attached at the robot table ${}^{\mathrm{B}}T_{\mathrm{RM_T}}$. By tracking this marker, the robot can be freely positioned relative to the corpse so that the needle can reach any target in the corpse. Lastly, we use a hand held pointer which is tracked by the tracking camera to define the needle tip position and orientation w.r.t. to the reflective markers at the EE ${}^{\mathrm{RM_{EE}}}T_{\mathrm{N}}$.

Using the chain of transformation from Figure 1, a desired target in the CT image coordinate system ${}^{\mathrm{CT}}\mathrm{DT}$ can be transformed into the coordinate system of the robot base according to

$$\begin{aligned} {}^{\mathrm{B}}T_{\mathrm{DT}} = {}^{\mathrm{B}}T_{\mathrm{RM_T}}\left({}^{\mathrm{C}}T_{\mathrm{RM_T}}\right)^{-1}{}^{\mathrm{C}}T_{\mathrm{RM_{CoReg}}} \\ {}^{\mathrm{RM_{CoReg}}}T_{\mathrm{CTM}}\left({}^{\mathrm{CT}}T_{\mathrm{CTM}}\right)^{-1}{}^{\mathrm{CT}}\mathrm{DT}. \end{aligned} \tag{1}$$

The desired EE position to reach the target with the needle can be calculated as

$${}^{\mathrm{B}}T_{\mathrm{EE}} = {}^{\mathrm{B}}T_{\mathrm{DT}}\left({}^{\mathrm{RM_{EE}}}T_{\mathrm{N}}\right)^{-1}\left({}^{\mathrm{EE}}T_{\mathrm{RM_{EE}}}\right)^{-1} \tag{2}$$

Data acquisition

The workflow for a robot guided biopsy is the following: first, the co-registration marker is placed loosely on the corpse. Next, a CT-scan (slice thickness 0.8 mm, lateral voxel size 0.65 mm) is acquired. The resulting DICOM is imported to our custom software. Based on a 3D visualization of the CT image the user is able to select the desired target including the orientation of the needle path. The software automatically identifies the pose of the CT Marker w.r.t. the CT-imaging system ${}^{\mathrm{CT}}T_{\mathrm{CTM}}$ by thresholding the CT image and finding the steel balls which belong to the checkerboard pattern. The ambiguity of the pose due to the symmetric steel ball pattern is resolved by considering the positions of the reflective markers which are also visible in the CT. Next, the poses ${}^{\mathrm{C}}T_{\mathrm{RM_{CoReg}}}$ and ${}^{\mathrm{C}}T_{\mathrm{RM_T}}$ are obtained from the tracking camera. Until this point, the co-registration marker is not allowed to move. With Eqs. (1) and (2) we can calculate the desired position for the robot and an initial position that represents the start of the needle path. We performed needle insertions in wax phantoms (n=28) and in the livers of two cadavers (n=10). We used G18 biopsy needles with a bevel tip and a length of 150 mm. For the purpose of defining insertion targets and retrieving them, we inserted small fiducials (steel balls, r=1 mm) into the wax phantoms and cadaver livers respectively with a hollow needle (see Figure 2).

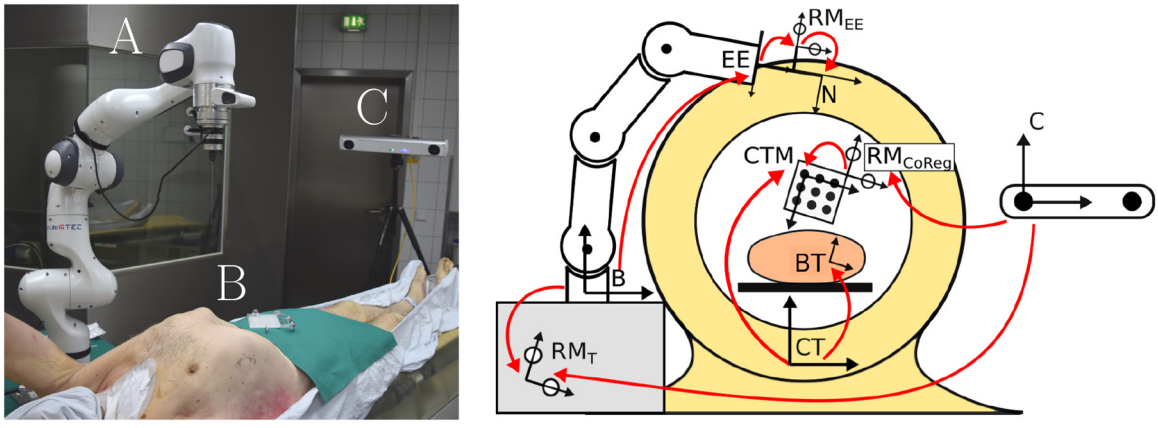

Figure 1: *Left*: Setup for performing needle insertions in a corpse. The biopsy needle is fixed to a robot (A). The co-registration phantom (B) is positioned on the corpse prior to CT scanning. The transformation matrix between the world reference system (not visible in the image) and the co-registration phantom is estimated with a tracking camera (C). *Right*: Registration of CT image and robot reference frame *Rb*. The position of the needle tip in the CT reference frame can be determined via the co-registration phantom.

Figure 2: *Left*: Wax phantom with implanted steel ball markers as targets. *Center*: Biopsy needle insertion into the liver of a corpse. The biopsy needle can be easily fixed and removed from the robot during placement with a drill chuck. *Right*: CT-image after needle insertion.

Evaluation

After the robot had performed each needle insertion, we unscrewed the needle from the chuck and removed the robot. Subsequently, another control CT scan was performed to determine placement accuracy. For this purpose, we detect needles by first thresholding the CT image and then finding connected components which represent needles based on the ratio of their principal axis lengths. For each needle, the position of its tip is determined as the voxel furthest away from the center in the direction of the first principal axis. For all needle insertions, we calculate position and orientation errors between planned needle pose and actual needle geometry in the control CT.

Results

The results for the needle placement accuracy in wax phantoms and livers of corpses are shown in Figure 3. Each insertion is depicted with its position and orientation error. For the wax phantoms, the mean position error is 4.34 ± 1.27 mm and the mean orientation error is 2.24 ± 0.63°. For the insertions into corpse livers the mean position error is 10.81 ± 4.44 mm and the mean orientation error is 4.29 ± 1.66°. During one insertion procedure, the needle came in contact with a rib. We consider this insertion as an outlier and excluded it from the calculation of the mean statistics. Insertion distance was 37.19 ± 5.05 mm through wax and 92.57 ± 14.89 mm through tissue.

Discussion and conclusion

The needle placement accuracy is influenced by multiple sources of errors. First, our approach involves three calibrations, each associated with an individual error:

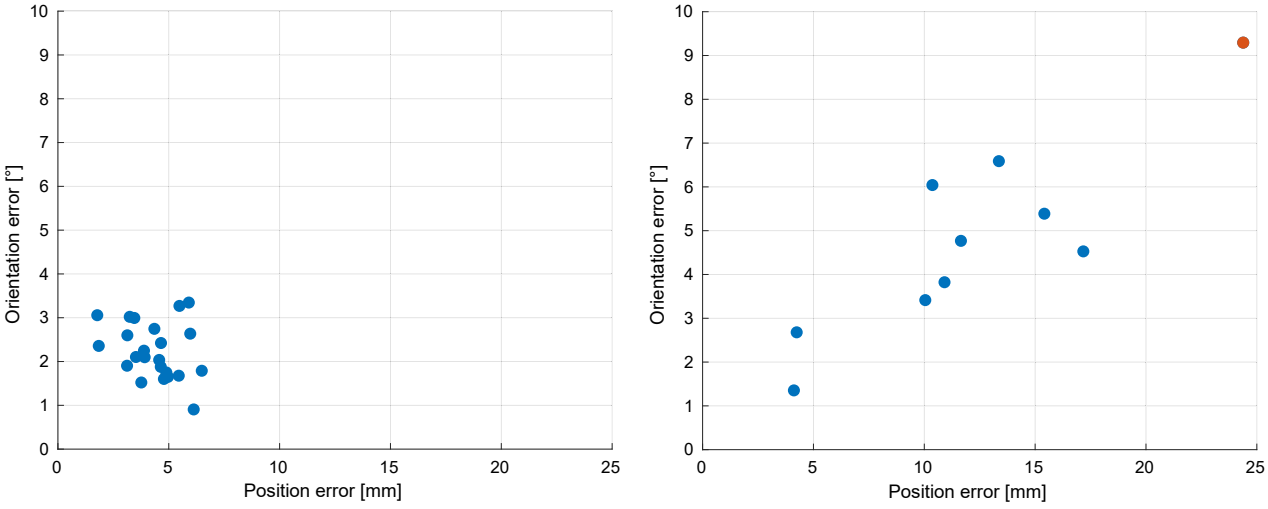

Figure 3: Needle placement accuracy for the insertion experiments. *Left*: Wax phantoms (n=28), *Right*: Corpse livers (n=10). The insertion colored in red is considered as an outlier.

estimation of the transformation within the co-registration marker ${}^{\mathrm{RM}_{\mathrm{CoReg}}}T_{\mathrm{CM}}$, hand-eye calibration of tracking camera and robot, and calibration of the needle w.r.t. the marker at the end effector ${}^{\mathrm{RM}_{\mathrm{EE}}}T_{\mathrm{N}}$. During the insertion, the needle can be deflected from the planned path, i.e. we observed that the needle is directed according to the inclined bevel tip. After the insertion, the needle is manually unscrewed which can cause its movement in the tissue. Lastly, the detection of the co-registration marker (subpixel accuracy) and the inserted needles (pixel accuracy) in the CT images contribute to the overall error. From the placements accuracy in wax phantoms we can conclude an upper bound for the sum of all calibration errors. This accuracy is comparable to existing CT based biopsy systems such as [6], where an accuracy of (3.2 ± 1.9 mm) was reached in a phantom study.

Mean error and standard deviation are larger for insertions into corpse livers compared to insertions into wax phantoms. As all error sources except for the needle-tissue interaction remain the same between these experiments, we conclude that this error component is responsible for the difference in needle placement accuracy. Its increased influence could result from a larger insertion distance and the fact that the real tissue is more firm compared to wax which both lead to a larger deflection of the needle in the direction of the bevel tip. The correlation between position and orientation error for the corpse experiments (Figure 3, right) supports this hypothesis.

In conclusion, we presented an approach to automated robotic biopsies which main advantage is its flexibility in the autopsy workflow. The robot can be placed freely and perform multiple biopsies in different body parts prior to a CA. Additionally, our approach does not require any online calibrations so that multiple punctures can be executed time efficiently. Our results show that the accuracy is sufficient for e.g. the puncture of larger blood calves. Further work should address compensating for the needle-tissue interaction, i.e. by rotating the inclined needle tip during the insertion based on force measurements at the needle shaft.

Acknowledgements: We thank the company mandel + rupp medizintechnik GmbH for kindly providing us the biopsy needles that were used in the experiments.
Research funding: This work was partially funded by DFG grants SCHL 1844/2-1 and SCHL 1844/2-2.
Author contributions: All authors have accepted responsibility for the entire content of this manuscript and approved its submission.
Conflict of interest: Authors state no conflict of interest.
Ethical approval: The research related to human use complies with all the relevant national regulations, institutional policies and was performed in accordance with the tenets of the Helsinki Declaration, and has been approved by the ethics committee of the Medical Center Hamburg-Eppendorf.

References

1. Park JP, Kim SH, Lee S, Yoo SH. Changes in clinical and legal autopsy rates in Korea from 2001 to 2015. J Korean Med Sci 2019; 34. https://doi.org/10.3346/jkms.2019.34.e301.
2. Kuijpers CC, Fronczek J, van de Goot FRW, Niessen HWM, van Diest PJ, Jiwa M, et al. The value of autopsies in the era of high-tech medicine: discrepant findings persist. J Clin Pathol 2014;67:512–9.
3. Latten B, Bakers F, Hofman P, zur Hausen A, Kubat B. The needle in the haystack: histology of post-mortem computed tomography guided biopsies versus autopsy derived tissue. Forensic Sci Int 2019;302:882.
4. Ben-David E, Shochat M, Roth I, Nissenbaum I, Sosna J, Goldberg SN, et al. Evaluation of a ct-guided robotic system for precise percutaneous needle insertion. J Vasc Intervent Radiol 2018;29: 1440–6.
5. Podder TK, Beaulieu L, Caldwell B, Cormack RA, Crass JB, Dicker AP, et al. Aapm and gec-estro guidelines for image-guided robotic brachytherapy: report of task group 192. Med Phys 2014;41:101, 501.
6. Ebert L, Ptacek W, Naether S, Fürst M, Ross S, Buck U, et al. Virtobot – a multi-functional robotic system for 3D surface scanning and automatic post mortem biopsy. Int J Med Robot Comput Assist Surg MRCAS 2009;6:18–27.
7. Ernst F, Richter L, Matthäus L, Martens V, Bruder R, Schlaefer A, et al. Non-orthogonal tool/flange and robot/world calibration. Int J Med Robot Comput Assist Surg 2012;8:407–20.